SLAC-PUB-15653
July 1, 2013

HOM DAMPING COUPLER DESIGN FOR THE 400-MHZ RF DIPOLE COMPACT CRAB CAVITY FOR THE LHC HILUMI UPGRADE*

Zenghai Li[1] and Lixin Ge, SLAC, Menlo Park, CA 94025, USA
J. R. Delayen and S. U. de Silva, Center for Accelerator Science, Old Dominion University, Norfolk, VA 23529, USA

Abstract

Crab cavities are adapted as the baseline design for the LHC HiLumi upgrade to achieve head-on beam-beam collisions for further improvement in luminosity. A 400-MHz compact RF dipole crab cavity design was developed by a joint effort between Old Dominion University and SLAC under the support of US LARP program. This design has shown very favorable RF parameters and can fit into the available beamline spacing for both vertical and horizontal crabbing schemes. A niobium proof-of-principle cavity based on such a design has been manufactured for vertical test. In addition, there are stringent wakefield requirements that needed to be met for such a cavity in order to preserve the quality of the circulating beams. In this paper, we will discuss different damping schemes for such a compact design and present the HOM coupler designs to meet the damping requirements.

INTRODUCTION

A crabbing scheme [1] has been adopted as the baseline tool for the LHC HiLumi upgrade. The nominal scheme for the HL-LHC is the local crabbing with the 400 MHz superconducting deflecting cavities. In the local crabbing scheme, the transverse size of the crab cavity is limited to 145-mm due to a small beam line separation. A conventional elliptical cavity at 400-MHz would not fit. To meet such a space constraint, an RF dipole (RFD) cavity [2-4] is being developed by a SLAC and ODU joint effort. The RFD design in concern is shown in Fig. 1. It consists of a square tank and two ridged deflecting poles. The operating mode is the TE11-like dipole mode. The deflection is mostly due to the electric field. Table 1 lists the major dimensions and RF parameters of the cavity. The RFD design is compact and low in surface field. In addition, there is no lower order mode. The lowest HOM is more than 230 MHz higher than the operating mode, which is advantageous for the design of HOM damping schemes. The present design also incorporates a curved pole profile as shown in Fig. 1 to improve the field uniformity within the beam aperture.

HOM damping is essential to maintain beam stability. In this paper we present the HOM and FPC coupler designs for the RFD cavity. We also present the multipacting analysis and mitigation to improve the cavity performance.

* This work was supported by DOE Contract No. DE-AC02-76SF00515 and was partially supported by the DOE through the US LHC Accelerator Research Program (LARP). Computations used computer resources at NERSC, LBNL.
[1]lizh@slac.stanford.edu

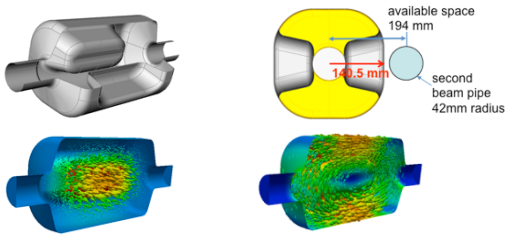

Figure 1: RF dipole (RFD) crab cavity and the electric and magnetic field patterns of the deflecting mode.

Table 1: Crab cavity RF parameters.

Frequency (MHz)	400
Operating Mode	TE11
Lowest dipole HOM (MHz)	633
Lowest acc HOM	715
Iris aperture (diameter) (mm)	84
Transverse dimension (mm)	281
Vertical dimension (mm)	281
Longitudinal dimension (w/o couplers) (mm)	556
R_T (ohm/cavity)	433
.V_T (MV/cavity)	3.34
Bs (mT)	55.6
Es (MV/m)	33.4

HOM COUPLERS

The HOM mode spectrum calculated using Omega3P [5,6] up to 2 GHz frequency is shown in Fig. 2. Notice that all the HOM frequencies are well above that of the operating dipole mode. The first HOM is a horizontal dipole mode at 633 MHz. The first important accelerating mode is at 758 MHz and the first vertical dipole mode at 776 MHz.

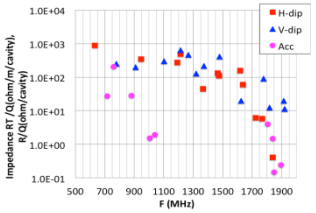

$$\frac{R_{shunt}}{Q} = \frac{|V_z|^2}{\omega U}$$

$$\frac{R_T}{Q} = \frac{\omega}{c}\left(\frac{|V_z(r_0)|^2}{\omega U (r_0\omega/c)^2}\right)$$

Figure 2: Mode spectrum.

The coupler design needs to meet the following space and RF considerations: 1) be clear of the second beam line which is 194 mm away; 2) all coupler ports point to the same direction to simplify the cryostat design; 3) the HOM couplers be able to handle large power generated by the beam due to the accelerating HOMs. The beam (σ_z=76 mm) induced power by the first major

accelerating mode at 750 MHz (R/Q~200) can be estimated as $48 I_b^2 Q_{ext}$. As an example, a half-ampere beam would produce a power of 6 kW for a Q_{ext} of 500. Thus a lower Q_{ext} is desirable even though beam breakup can tolerate a larger Q_{ext}.

Horizontal HOM coupler (deflecting plane)

The horizontal HOMs are damped via a ridged waveguide coupler as shown in Fig. 3. The coupler waveguide has a cutoff of around 560 MHz so that the operating mode at 400 MHz will not propagate. Using a ridged waveguide design, the size of the coupler is reduced by half (135 mm vs 270 mm as compared with a rectangular geometry). The coupler couples to the cavity via a rectangular slot on the end plate of the cavity. Any mode that has a magnetic field in the direction of the slot will be damped. So this coupler is effective for both the horizontal HOMs and the accelerating HOMs. Simulation has shown that one such coupler is sufficient to provide the required damping. To maintain the field symmetry, a symmetrizing stub is attached on the opposite side, which is later used for the FPC coupler (see below).

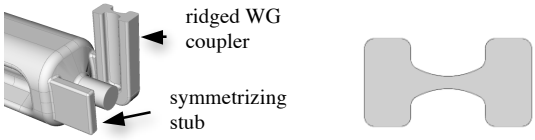

Figure 3: Ridged waveguide coupler for the horizontal and accelerating HOMs. Right) waveguide cross section.

Vertical HOM coupler

The vertical HOM coupler consists of a waveguide stub and a coaxial pickup as shown in Fig. 4. The coupler does not couple to the operating mode because the slot is perpendicular to the magnetic field, so that no filter is needed. The coupler couples to both the vertical and the accelerating HOMs. The asymmetry of the waveguide stub and the coax pickup position were designed to couple to the quadrupole and higher multipole HOMs. The indentation on the wall of the waveguide stub is to enhance coupling.

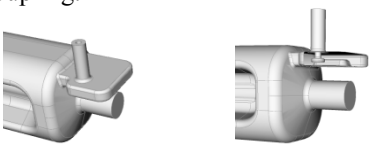

Figure 4: Selective coupler for the vertical HOM.

HOM Damping results

Fig. 5 shows the damping of three typical HOMs by the horizontal and vertical couplers. The Qext calculated using Omega3P for modes up to 2 GHz is plotted in Fig. 6 (left). The impedances of the HOMs ((R/Q)*Qext) are summarized in Fig. 6 (right). The solid lines are the impedance budget for dipole HOMs (blue) and accelerating HOMs (purple) respectively. All the modes are damped to well within the impedance requirement, except for the two vertical modes at 1.27 and 1.48 GHz. More optimization of the vertical coupler is under way to resolve these high Q modes.

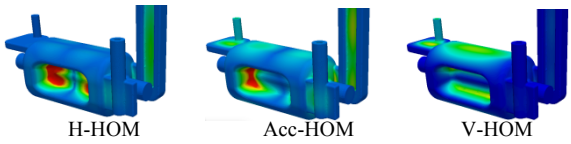

Figure 5: Damping of HOMs via HOM couplers.

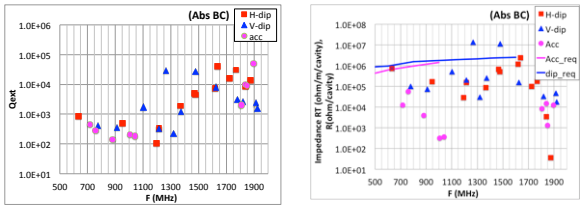

Figure 6: The Qext and impedance of the HOMs.

FPC COUPLER

The symmetrising stub (opposite to the HOM coupler) is used as the coupling port to the cavity as shown in Fig. 7. The waveguide stub is adapted to a coaxial waveguide that leads to the main assembly of the coaxial coupler. The coaxial waveguide has an inner conductor diameter of 27 mm and outer conductor diameter of 62mm, the same as the coaxial coupler for the LHC main cavity, and it is orientated in the same direction as the other HOM couplers so that the cryostat vessel only has port interfaces on one side of the surface. The coaxial waveguide is parallel to the E-plane of the waveguide stub but with the coaxial center-line off the symmetry plane of the stub to achieve a finite coupling. The coupling is further enhanced with a hook-shaped probe. The spacing between the hook-probe and the waveguide wall is fixed at 10 mm. The coupling can be adjusted by varying the vertical position of the probe. Fig. 7 shows the Qext as a function of tip position for two slightly different probe shapes. The required coupling is 10^6 which is readily achievable with such a FPC design.

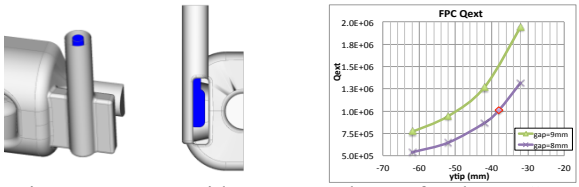

Figure 7: Waveguide to coax adaptor for the FPC.

MP SIMULATION USING TRACK3P

Multipacting (MP) analyses were carried out using Track3P [7]. The field level was scanned up to 6 MV of deflecting voltage with a 0.25 MV interval. At each field level, 50 RF cycles were simulated for obtaining the parameters of the resonant trajectories. The MP strength is estimated using the impact energy and the SEY curve. A typical SEY curve for niobium is shown in Fig. 8 which has a peak SEY at around 300 eV.

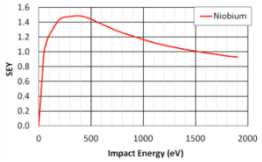

Figure 8: SEY dependence on impact energy for Niobium.

MP in the ridged waveguide HOM coupler

Simulation using Track3P has unveiled a significant MP band in the ridged gap as shown in Fig. 9. At a given field level, there is a finite region along the waveguide that supports resonant trajectories. Due to the evanescent nature of field distribution, the MP region shifts along the waveguide as the field level varies. The impact energies of the resonant trajectories are in the range of high SEY. Strong MP are expected at all field levels.

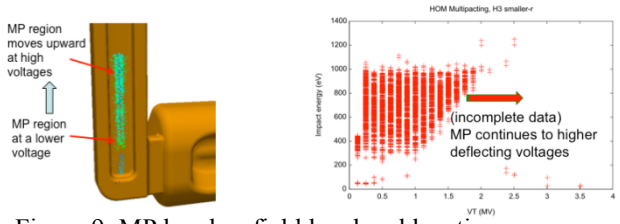

Figure 9: MP band vs field level and location.

Mitigation methods were studied to suppress the resonant trajectories. Grooves with different slanted angles were tested and were found not effective (mainly due to limited groove depth in a small gap).

The effective MP suppression was realized by increasing the curvature of the gap surface. With a larger curvature, the field becomes much less uniform which reduces the MP area to a narrow region around the center of the gap. The MP area is further eliminated by an additional small bump as shown in Fig. 10.

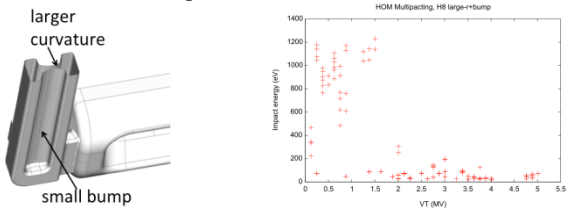

Figure 10: Ridged gap surfaces with a larger curvature significantly reduce the MP region. A small bump further eliminates the MP resonances.

MP in the FPC coupler

There were no significant MP trajectories found in the region of the waveguide to coax adaptor. There are some resonant trajectories in the coax waveguide, which are not expected to be strong MP due to high impact energies.

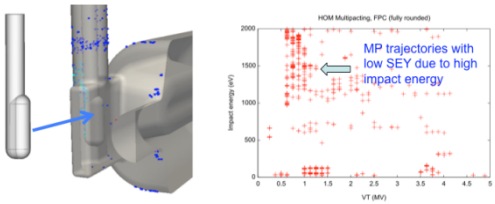

Figure 11: MP in the FPC coupler.

MP in the vertical HOM coupler

There is no MP trajectories found in the vertical HOM coupler region because the coupler does not couple to the deflecting mode and there is virtually no field in the coupler.

MP in the cavity

There are three MP bands below 3 MV deflecting voltage as shown in Fig. 12, which can have larger than unity secondary electron yield. These resonances are located on the end plate of the cavity. These MP bands were confirmed in the high power testing of a prototype cavity of a similar design and were successfully processed without much difficulty [8].

There is a MP band in the cavity at voltage levels 3 MV and up. The impact energies of the electrons in this band are much lower than the impact energy of the peak SEY, and hence it is not expected to be a strong barrier.

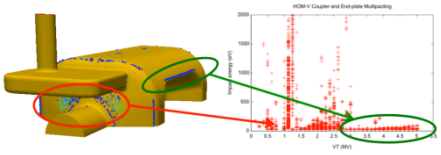

Figure 12: MP inside the cavity.

SUMMARY

The RFD crab cavity was optimized. Curved pole profile was incorporated in the design to minimize the multipole fields. A ridged waveguide HOM coupler, for the horizontal HOMs, and a selective HOM coupler, for the vertical HOMs, were presented. Strong damping was obtained for the dipole HOMs as well as the accelerating HOMs. A waveguide-to-coax adaptor FPC coupler was designed, utilizing the symmetrizing stub as a coupling port. Multipacting analyses were carried out. Strong multipacting resonances in the HOM coupler were eliminated via shape optimization. The design has been provided for the cryostat engineering design.

REFERENCES

[1] https://twiki.cern.ch/twiki/bin/view/Main/LHCCrab Cavities

[2] J. R. Delayen and S. U. de Silva, "ODU/JLAB Parallel-Bar Cavity Development," US LARP Collaboration Meeting, Montauk, NY, May 2011.

[3] Zenghai Li and Lixin Ge, "Compact Crab Cavity for H and V Crabbing," US LARP Collaboration Meeting, Montauk, NY, May 2011.

[4] Zenghai Li, et al., "RF Modeling Using Parallel Codes ACE3P for the 400-MHz Parallel-bar/Ridged-waveguide Compact Crab Cavity for the LHC HiLumi Upgrade," Proc. IPAC2012, New Orleans.

[5] K. Ko, et al., "Advances in Parallel Computing Codes for Accelerator Science and Development," Proc. LINAC2010, Tsukuba, Japan, 2010.

[6] Lie-Quan Lee, et al., Omega3P: A Parallel Finite-Element Eigenmode Analysis Code for Accelerator Cavities, SLAC-PUB-13529, 2009.

[7] L. Ge, et al., "Multipacting Simulations of TTF-III Power Coupler Components," Proc. PAC07, Albuquerque, New Mexico.

[8] J. Delayen, et al., "Proof-of-Principle cavity preparation and testing, RFD cavity", LARP CM20, Napa, CA, 2013; and S. U. De Silva et al, paper WEPWO080, this conference.